Desalination and Water Treatment
www.deswater.com

doi: 10.1080/19443994.2015.1096831

57 (2016) 19292–19300
September

Taylor & Francis
Taylor & Francis Group

Photocatalytic degradation of methyl blue by tourmaline-coated TiO_2 nanoparticles

Xuesen Bian[a], Rong Ji[b,*]

[a]*Nanjing Institute of Environmental Sciences of the Ministry of Environmental Protection of China, 8 Jiangwangmiao Street, Nanjing 210042, P.R. China*
[b]*School of the Environment, Nanjing University, 163 Xianlin Avenue, Nanjing 210046, P.R. China, Tel. +86 13160075092; email: njudoc@163.com*

Received 25 February 2015; Accepted 12 September 2015

ABSTRACT

Complex photocatalysts were prepared by coating TiO_2 nanoparticles with tourmaline and used in the photocatalytic degradation of simulated methyl blue wastewater. The photocatalytic activities and crystalline form were affected by the synthetic conditions, with the optimum catalyst preparation of using 1% in weight, of HCl treated tourmaline passed by the 3,000 mesh sieve, and finally calcination at 450°C for 5 h. The addition of SO_4^{2-} or lowering of solution pH decelerated photocatalytic degradation, while cations like Ca^{2+}, Zn^{2+}, and Mg^{2+} accelerated the reaction. Results of our study indicate that tourmaline due to its broadening utilization potential is a helpful carrier to enhance the effect of the TiO_2 photocatalytic method in the processing of dye wastewater.

Keywords: Tourmaline; TiO_2; Coat; Photocatalysis; Hydroxyl radical

1. Introduction

Dye production occupies an important part in industries worldwide. It was estimated that the global output of dyes can be as large as about 1,280,000 tons in the year of 2012 [1], among which 1–2% during manufacturing and 1–10% during usage are released directly into the environment [2]. Thus, the potential hazards of various dyes, as common organic pollutants, have become a focus of environmental researchers [3,4]. Besides, wastewater from the dye industry is highly visible and complex in composition, thus representing a source of pollution in need of special attention [5]. Till now, treatment of dye wastewater can be divided into physical, biological, and chemical methods. The physical treatment, represented by adsorption, coagulation, and filtration, usually removes only pollutants from one phase to another without entirely decomposing them, and thus the secondary source of pollution still needs to be treated. On the other hand, complex aromatic structures commonly existing in dye chemicals often lead to their stability, to be resistant to biodegradation [6]. Therefore, chemical processes like heterogeneous photocatalysis, Fenton oxidation, ozone treatment, and ultrasonic decomposition are usually considered as effective ways in the entirety of removal with reduced hazards to environment. Photocatalysis is a novel method which attracts vast interest in the last few years [7]. Research of the photocatalytic method, represented by TiO_2 photocatalysis, especially draws a lot of interest due to its innocuity, reusability of catalyst as well as the vast

*Corresponding author.

applicability towards a wide variety of pollutants. The degradation mechanism is usually explained as follows: the n-type semiconductor of TiO_2 absorbs photon-holding energy equaling to or more than its band gap and the electron transits from the valence band to the conduction band leaving the electron and the hole separated. Holes can either oxidize the organic pollutants directly or react with H_2O molecules to form ·OH radicals, which can nearly degrade any organic chemicals in solutions unselectively due to their strong oxidizability. The photogenerated electrons may also react with water-dissolved oxygen and H^+ to form H_2O_2, which can further be decomposed by light to ·OH radicals. Till now, the low-quantum yield arisen by the easy recombination of photogenerated holes and electrons still limits the further widening of practical utilization of photocatalytic techniques.

Tourmaline is a common natural mineral widely distributed in China. Since the discovery of its spontaneous electric field, this mineral has been utilized in fields like medical treatment, improvement of water quality, and purification of air. The investigation for its photochemical usage was once carried out by some researchers to employ it as an iron source of Fenton reagent [8,9] and it could also be used as photocatalyst alone, according to our previous study [10]. The existence of electric field can help separate holes and electrons. Thus, the mineral may be able to coat TiO_2 nanoparticles to result in a better isolation of photogenerated holes and electrons, and thus to better enhance the quantum yield compared to traditional carriers. The enhancement of TiO_2 photocatalytic activity by tourmaline was reported by some previous researchers [11,12]. This study is designed to prepare tourmaline–TiO_2 composite photocatalyst using the sol–gel method to explore the optimum synthetic condition and to investigate the effects of common environmental factors of wastewater on the final removal rate.

2. Experimental

2.1. Materials

Methyl blue (MB) was bought from Sigma. The mobile phase of HPLC was of chromatographic grade, while other chemicals were of analytical grade and were used without further purification. Fe-tourmaline was purchased from Chuanshi mineral processing factory, Hebei, China.

2.2. Instrument

The photoreactor was designed according to the following description. A hollow column tube was used as the reaction container with two open gaps in opposite directions in its upper part: one for the input of air and the other for the injection of samples. A straight internal tube was inserted to hold the ultraviolet lamp (254 nm, 13 W), which was purchased from the Xujiang Electromechanical Plant, Nanjing, China. Water for cooling the lamp was continuously flowing through the closed area of the internal pipe during the whole process of the reaction.

The HPLC system used in this study was an Agilent 1200 series HPLC system, which consisted of a G1322 A degasser, a G1311 A Quat Pump, a G1329 A thermostatted autosampler, a G1316A column oven, and a G1314A DAD detector. The column used for the separation was Agilent Eclipse XDB-C18 (5 μm, 4.6 × 250 mm). The X-ray diffractometer used was from X'TRA with CuKα irradiation.

2.3. Pretreatment of tourmaline powder

The crude tourmaline powder was firstly passed through a 3,000-mesh sieve. After that, it was dispersed in double-stilled water with ultrasonic for 1 h. Then, the filtered powder was immersed for 24 h in solutions, whose pH was adjusted to 1.00 by acids or to 12.00 by bases. After that, it was washed repeatedly with double-distilled water till the supernatant turned neutral. Finally, the powder was separated out and dried at 80°C.

2.4. Synthesis of tourmaline-coated TiO_2

9 mL of tetrabutyl titanate (TBOT) was mixed with 90 mL of ethanol and a certain weight of treated tourmaline was added by stirring for 20 min. After that, a mixture containing 10 mL of ultrapure water, 5 mL of HCl, and 20 mL of ethanol was dripped carefully into the system till the pH turned to 0.8. The stirring was kept for 24 h at room temperature. 1 mol L^{-1} $NH_3{\cdot}H_2O$ was then dripped in till the gel was formed. After being aged for 3 h, the gel was dried at 110°C and calcined at certain temperatures in a muffle oven.

2.5. Photocatalytic degradation of MB

About 11 mg L^{-1} MB solution was prepared by dissolving 5.5 mg of MB into 500 mL of ultrapure water, which was then transferred into the reaction container. The liquid depth in the reactor reached approximately 7.1 cm. After that, chemicals for investigation into the effects of factors were introduced in and 260 mg L^{-1} photocatalyst was added. The first sample was taken by injection after 1 h of magnetic stirring of the suspension. The 13-W, 254-nm

ultraviolet lamp in the central hollow part of the internal tube was then turned on, and photocatalytic degradation started. All experimental processes were accompanied by vigorous stirring and air pumping into the system at 1 mL s^{-1}. Samples were all extracted by a 10-mL injector, centrifuged (10,000*g*, 8 min), and the supernatants were separated to be stored at −20˚C. All experiments were performed at least in duplicate.

2.6. HPLC analysis and characterization of photocatalyst

The mobile phase used for the analysis of MB was acetonitrile:water = 30:70 (v:v) isocratically running at a rate of 1 mL min^{-1}. Determination of MB was performed selecting 614 nm as the detection wavelength. The XRD characterization of tourmaline and TiO_2 complex photocatalysts was done under the following conditions: the tube voltage and current were 40 kV and 40 mA, respectively. 2θ was measured from 10 to 75˚ for tourmaline and from 20 to 80˚ for TiO_2 photocatalysts, respectively, with a step size of 0.02˚.

3. Results and discussion

3.1. The XRD characterization of tourmaline

The XRD result of Fe-tourmaline used in this study is shown in Fig. 1. 2θ values of 13.88˚, 20.96˚, 22.20˚, 30.14˚, and 34.66˚ are in accord with those from Meng et al. [12], demonstrating the characteristic peaks of Fe-tourmaline.

3.2. Effect of tourmaline treatment

Generally speaking, natural minerals are formed over very long periods of time and are complex in composition. To be suitable as carriers for catalysts, they were often pretreated before use. For instance, the pretreatment of wollastonite varied its surface coordination structure, raised the concentration of hydroxyls, diminished phase interface, and therefore enhanced the combination between the carrier and the photocatalyst [13]. The photocatalytic degradation curves by complex catalysts under different conditions are shown in Fig. 2. The photocatalytic degradation rates for MB can be approximated as pseudo-first-order kinetics, according to the Langmuir–Hinshelwood model. In this case, the photocatalytic degradation reaction rate equation could be reasonably described by a pseudo-first-order kinetics equation, $-dC/dt = kC$, where k is the pseudo-first-order reaction rate constant.

It can be learned from Fig. 2(a) that except TiO_2 loaded on NaOH-treated tourmaline, the photocatalytic activity of which was lower than pure TiO_2, four other treatments all resulted in different extents of enhancement of TiO_2 photocatalytic activity. The possible mechanism might be [12]: (i) the carrier helps increase the active sites of photocatalyst; (ii) the spontaneous electric field of tourmaline decelerates the recombination of photo-generated holes and electrons, which enhances the quantum yield; (iii) the far-infrared radiation and electric field effect of tourmaline may help to diminish the clustering of water molecules and thus enhance the concentration of OH^- in the system, which may also increase ·OH radicals in the system.

All five complex photocatalysts showed the character of anatase crystal (Fig. 3), while the peak of 2θ = 30.78˚ in the spectra of tourmaline treated by NaOH and H_2SO_4 corresponds to the brookite feature. Besides, peaks of both samples appear blunt compared to those of others, indicating worse crystallinity. The diameter of these particles can be estimated according to the Scherrer formula [14]: $D = K\lambda/\beta\cos\theta$, in which D

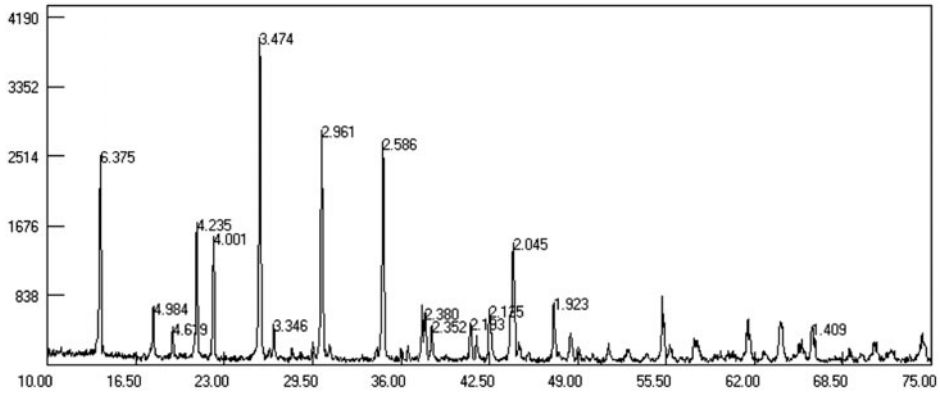

Fig. 1. XRD spectrum of tourmaline used in this study.

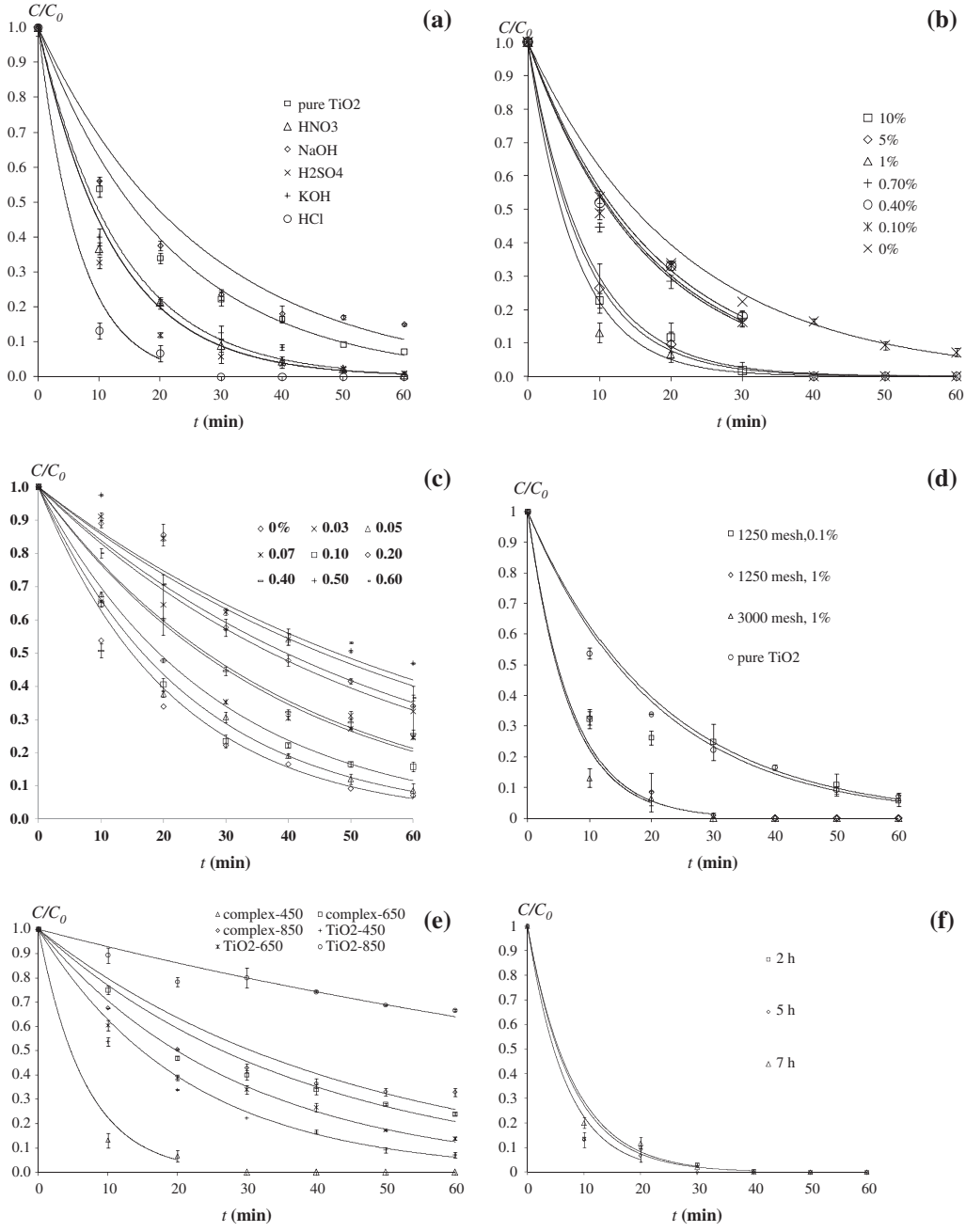

Fig. 2. Photodegradation of 11 mg L^{-1} MB in ultrapure water under UV 254 nm (13 W) as air was pumped in at 1 mL s^{-1} catalyzed by tourmaline–TiO_2 complex photocatalyst with different treatments: (a) effect of tourmaline processing, (b) effect of tourmaline content, (c) addition of untreated tourmaline, (d) effect of tourmaline size, (e) effect of calcination temperature, and (f) effect of calcination time.

is the diameter (nm); K is the Scherrer constant and often valued as 0.9; λ is the wavelength of X-ray, 0.1541 nm in this study; β is the width at the half peak; and θ is the Bragg diffraction angle. The peak top at $2\theta \approx 25.3$ was used for this calculation. The calculated D values were in the range of 10–20 nm. TiO_2 coated by base-treated tourmaline showed a lower photocatalytic activity than those coated by acid-treated tourmaline (Fig. 2(a)), which might suggest that the impurities in tourmaline surface tend to be more dissolved and removed by acid. Among the three acids, HCl treatment exhibited the best carrier effect, which entirely decolored the MB solution in 30 min^{-1} ($k = 0.149\ min^{-1}$, $R^2 = 0.91$) under

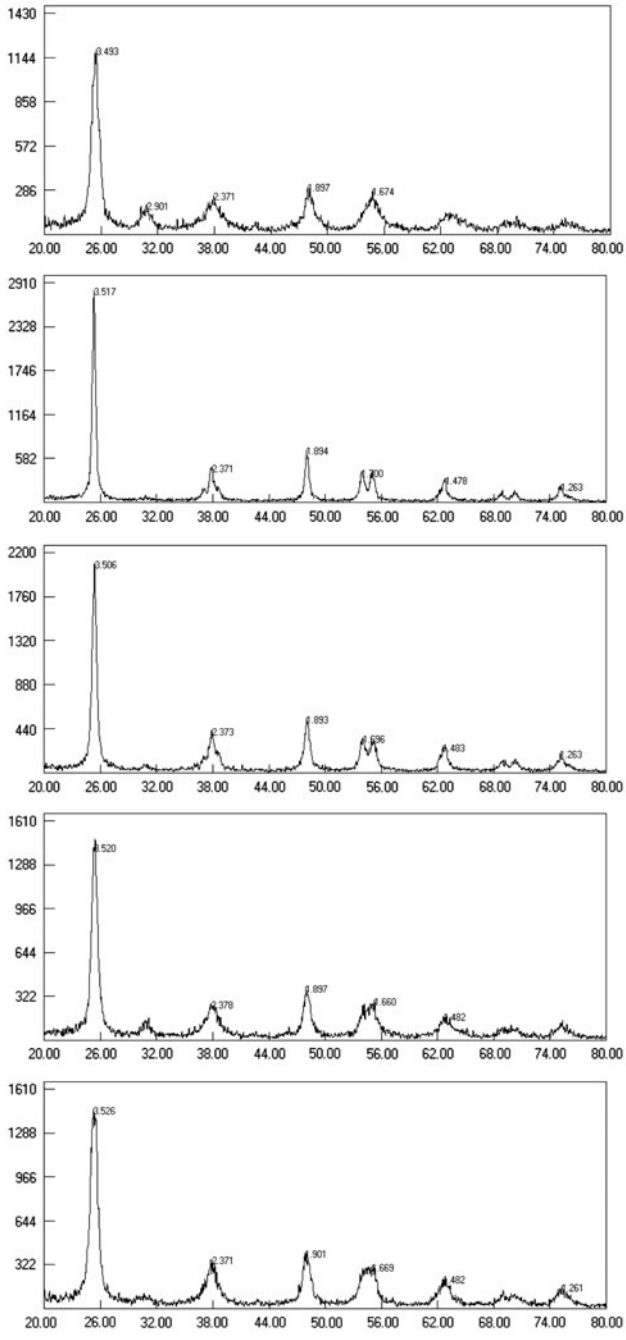

Fig. 3. XRD spectra of TiO_2 coated on tourmaline with different treatments, in the order downward from the top: NaOH, KOH, HNO_3, H_2SO_4, and HCl.

UV irradiation, thus was selected as the basis for further study.

3.3. Effect of tourmaline content

The optimum tourmaline usage was investigated by varying the weight of treated tourmaline powder added. A trend of peak broadening was observed in the XRD spectra (Fig. 4), suggesting the existence of tourmaline which helps to diminish the size of TiO_2 nanoparticles. It can be seen from Fig. 2(b) that in the ratio range of 0.1–10% of tourmaline weight, all of the complex photocatalysts showed a stronger activity than pure TiO_2. The photocatalysts containing 0.1–0.7% tourmaline were slightly more active than pure TiO_2, while the 1% tourmaline content exhibited the best removal effect ($k = 0.149\ min^{-1}$, $R^2 = 0.91$). Further enhancement of the tourmaline amount to ratios of 5 and 10% only led to a decreasing trend in photoactivity ($k = 0.121\ min^{-1}$, $R^2 = 0.99$, and $k = 0.122\ min^{-1}$, $R^2 = 0.97$, respectively). This might be explained as that the excessive tourmaline shadowed the irradiation of UV light to inhibit the contact of TiO_2 with photons. Besides, the amount of photocatalyst added remained constant, which meant that the increased amount of tourmaline led to the decrease in TiO_2 amount.

For comparison, the crude tourmaline powder was used to synthesize the complex photocatalyst using the same procedure. It can be learned from Fig. 2(c) that none of the addition levels resulted in the enhanced activity of TiO_2 photocatalyst, but in turn decreased the removal rate, the extent of which was turning larger as the content of tourmaline increased. Clearly, the untreated tourmaline within only masked the UV irradiation and reduced the effective TiO_2 amount. Therefore, the catalytic effects of the complex photocatalyst were decreased.

3.4. Effect of tourmaline diameter

For comparison, tourmaline powder filtered by a 1,250-mesh sieve was used to synthesize the complex photocatalyst using the same procedure. Fig. 2(d) shows that the tourmaline particle size can, to some extent, affect the carrier effect, while TiO_2 coated with 3,000-mesh-sieved tourmaline exhibited slightly higher activity ($k = 0.149\ min^{-1}$, $R^2 = 0.91$) than that sieved with 1,250 mesh ($k = 0.13\ min^{-1}$, $R^2 = 0.96$). This might indicate that tourmaline with a smaller size can be exposed more to TiO_2 nanoparticles, which enhances its carrier effect. The complex catalyst containing 1% 1,250-mesh tourmaline also showed a much higher activity than that of 0.1%, suggesting the tourmaline content is the key factor determining photocatalytic activity.

3.5. Effect of calcination temperature and time

It can be learned from Fig. 2(e) that photocatalytic activity decreased in the order of 450–650–850°C.

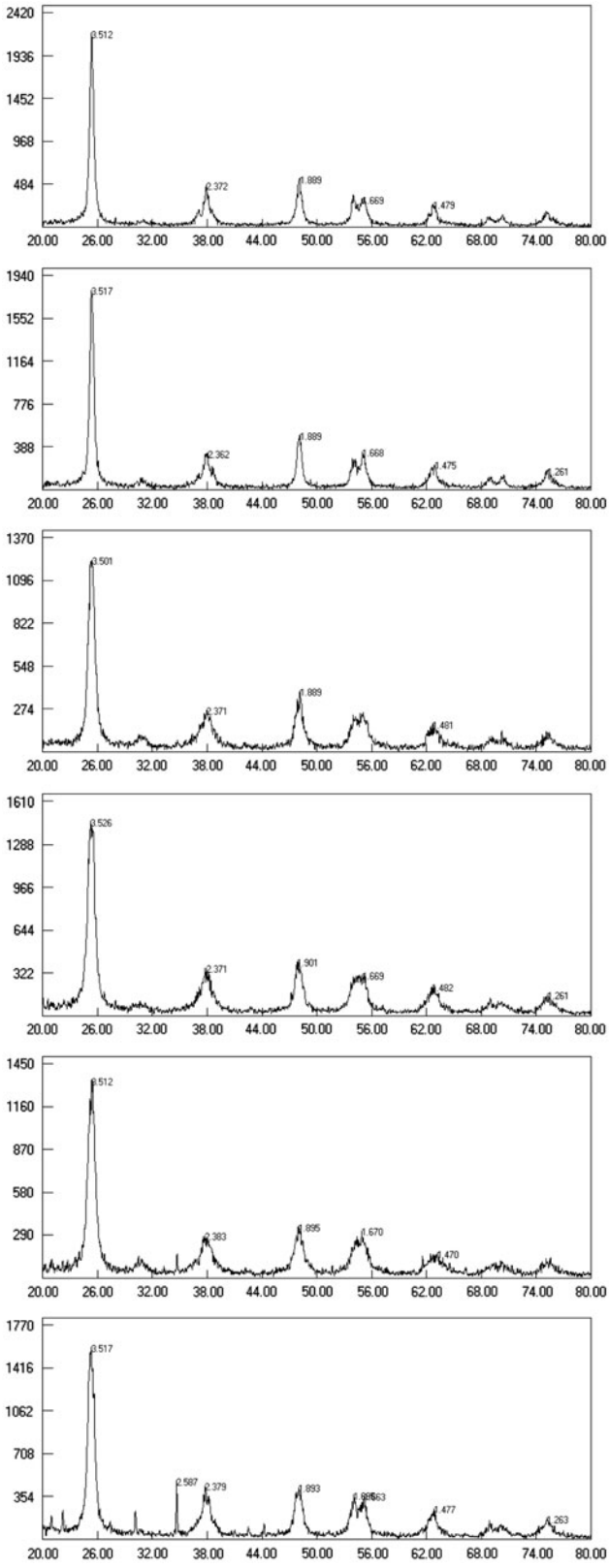

Fig. 4. XRD spectra of TiO_2 coated on different contents of HCl-treated tourmaline, in the order downward from the top: 0.1, 0.4, 0.7, 1, 5, and 10%.

Compared to pure TiO_2, the tourmaline-coated samples calcined at 450 and 850˚C showed a higher photoactivity, but at 650˚C, it is reversed. It is demonstrated that the formation and activity of photocatalyst are influenced by various factors in a complicated manner. Only when these factors, like spontaneous electric field and far-infrared radiation of tourmaline, are coordinated with the preparation conditions like the thermal effect, can the photocatalytic activity be enhanced by coating.

The complex photocatalysts were calcined at the set temperature of 450˚C for 2, 5, and 7 h, respectively. Obviously, 5 h of calcination resulted in the highest activity of complex photocatalyst (Fig. 2(f)). Sufficient calcination time is necessary for the optimal formation of crystalline, but excess heating also leads to the skeletal collapse of TiO_2 crystalline [15] as well as the unnecessary exhaustion of energy. Therefore, 5 h was selected as the calcination time for all other synthetic samples.

3.6. Adsorption and effect of environmental conditions of photocatalysis

The adsorption experiment was performed under the same conditions with photocatalysis but without UV irradiation. The adsorption ratio was 30 percent in 1 h by pure TiO_2, which was greatly enhanced when the catalyst contained 1 and 10% tourmaline with adsorption rates of 100 and 70% in half an hour, respectively. The catalyst containing 0.1%

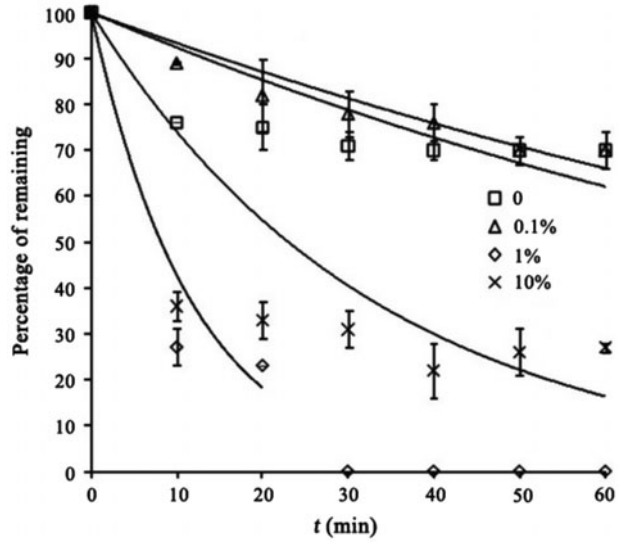

Fig. 5. Adsorption curves of 11 mg L^{-1} MB in ultrapure water by TiO_2 coated on different contents of tourmaline.

tourmaline showed a performance similar to that of pure TiO_2, with a slightly slower process in the beginning (Fig. 5). The mechanism of photocatalytic reaction in solutions is still not defined, and focused on whether the key reactants are photo-generated holes or hydroxyl radicals. Du et al. considered that the hydroxyl radicals may not play an important role once the decoloration rate is positively proportional to the adsorption rate [16], but Turchi and Ollis argued that after being formed, the hydroxyl radicals may be adsorbed on the catalyst surface and attack the organic molecule either adsorbed or distributed in solution; or diffuse to the solution and react with dissolved organic molecules [17]. ·OH may be spread as far as only 1 μm even if the solute concentration is as low as 10^{-6} mol L^{-1}, meaning that the hydroxyl radical reaction may also occur in solution near the catalyst surface [17]. Therefore, this phenomenon alone does not mean the assertion of any mechanism. The ethanol, commonly accepted as a hydroxyl scavenger, was thus added into the photocatalytic system, and inhibited the reaction to some extent (Fig. 6(a)). Therefore, ·OH plays an important role in this reaction.

The removal slowed down when the solution pH was adjusted to 3.54 by HCl. The acidic condition may decelerate the ionization of water molecule and fewer $^{-}$OH exist near the active sites of catalyst, thus decreasing the hydroxyl radicals derived from $^{-}$OH oxidation by holes [18]. The replacement of formic acid as the acidifier did not result in an even higher decelerating effect. Formic acid acts as the hole scavenger in a photolytic system [19]. If holes also played a key role in this system, the existence of formic acid

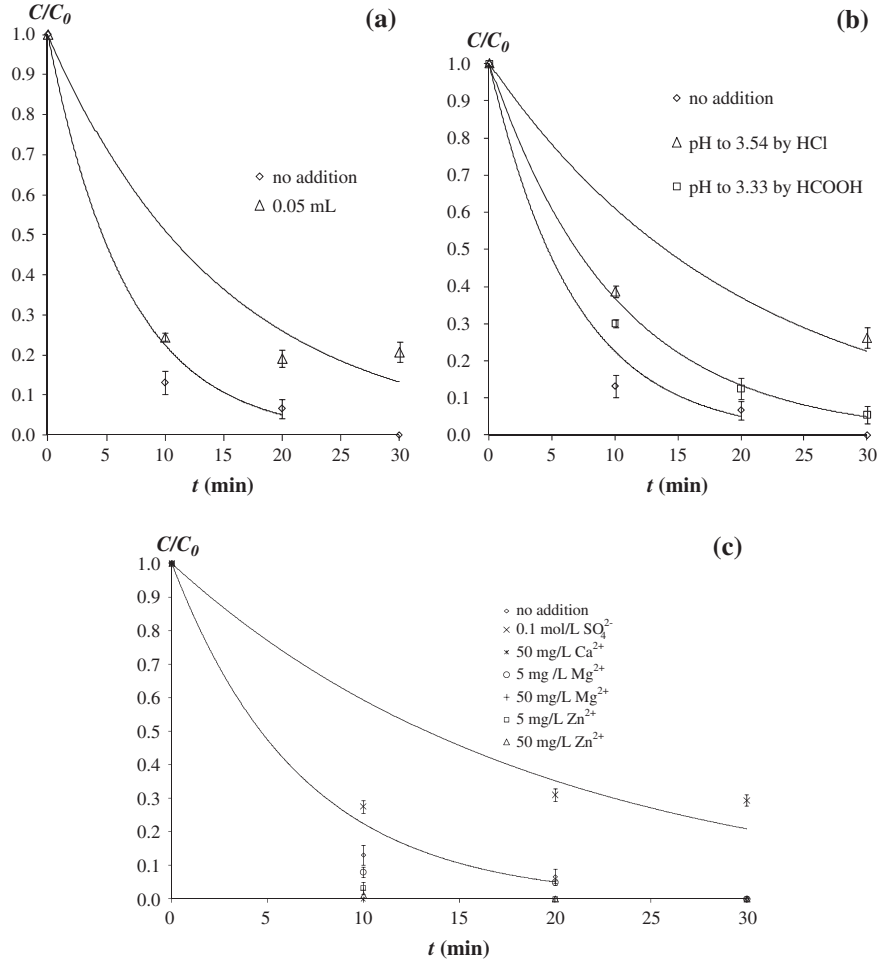

Fig. 6. Photodegradation of 11 mg L^{-1} MB in ultrapure water under UV 254 nm (13 W) as air was pumped in at 1 mL s^{-1} with tourmaline–TiO_2 photocatalyst under various environmental conditions: (a) effect of ethanol addition, (b) effect of pH value, and (c) effect of ions.

would have enhanced the inhibition effect. Therefore, it can be concluded that the reaction is mainly mediated by ·OH.

The addition of SO_4^{2-} decelerated the reaction as shown in Fig. 6(c). SO_4^{2-} in a photocatalytic system can be adsorbed on the surface of the photocatalyst and decrease its reactive sites [20].

The cations, like Ca^{2+}, Zn^{2+}, and Mg^{2+}, usually enhanced the photocatalytic removal rates according to some authors [21–23], most probably due to their absorption of photoelectrons. In our study, except the insignificant effect of 5 mg L^{-1} Mg^{2+} (k = 0.155 min^{-1}, R^2 = 0.93), other added metallic cations all accelerated the photocatalytic reaction to lead to the complete disappearance of MB in the solution within 20 min. Therefore, a little hardness may be beneficial to dye removal in wastewater by the photocatalytic method.

4. Conclusions

Tourmaline-coated anatase TiO_2 nanoparticles were prepared and investigated into photocatalytic activity using MB as the target removal pollutant. The optimum sol–gel synthetic reaction condition uses one percent weight HCl-treated tourmaline passed through the 3,000-mesh sieve and finally calcined at 450°C for 5 h. Photocatalysis took the main mechanism of hydroxyl mediation, and the enlargement of catalyst surface area, electric field as well as the far-infrared effect of tourmaline could be the main reason for the enhancement of photocatalytic activity. Existence of SO_4^{2-} or the acidified solution was not beneficial to the dye degradation, while cations like Ca^{2+}, Zn^{2+}, and Mg^{2+} enhanced the removal effect. The results of this study demonstrated that tourmaline can act as a helpful carrier to enhance the processing efficiency of dye wastewater using TiO_2 photocatalysis.

References

[1] Yubozhiye Market Research Center, Analysis of the General Situation and Status of the Chinese Dye Industry, 2014–2015. Available from: <http://www.chinabgao.com/k/ranliao/15555.html>.

[2] E. Forgacs, T. Cserháti, G. Oros, Removal of synthetic dyes from wastewaters: A review, Environ. Int. 30 (2004) 953–971.

[3] T. Platzek, C. Lang, G. Grohmann, U.S. Gi, W. Baltes, Formation of a carcinogenic aromatic amine from an azo dye by human skin bacteria *in vitro*, Hum. Exp. Toxicol. 18 (1999) 552–559.

[4] A.K. Mittal, C. Venkobachar, Sorption and desorption of dyes by sulfonated coal, J. Environ. Eng. 119 (1993) 366–368.

[5] K.Y. Foo, B.H. Hameed, An overview of dye removal via activated carbon adsorption process, Desalin. Water Treat. 19 (2010) 255–274.

[6] S. Wang, H. Li, Kinetic modelling and mechanism of dye adsorption on unburned carbon, Dyes Pigm. 72 (2007) 308–314.

[7] M. Habibi, A.A.L. Zinatizadeh, M. Akia, Photocatalytic degradation of Tire Cord manufacturing wastewater using an immobilized nano TiO_2 photocatalytic reactor, Desalin. Water Treat. (2014) 1–17.

[8] H. Xu, M. Prasad, Y. Liu, Schorl: A novel catalyst in mineral-catalyzed Fenton-like system for dyeing wastewater discoloration, J. Hazard. Mater. 165 (2009) 1186–1192.

[9] M. Tokumura, H.T. Znad, Y. Kawase, Modeling of an external light irradiation slurry photoreactor: UV light or sunlight-photoassisted Fenton discoloration of azo-dye Orange II with natural mineral tourmaline powder, Chem. Eng. Sci. 61 (2006) 6361–6371.

[10] X. Bian, J. Chen, R. Ji, Degradation of methyl blue using Fe-tourmaline as a novel photocatalyst, Molecules 18 (2013) 1457–1463.

[11] L.B. Liu, D.L. He, D.M. Zhao, Study on photocatalysis degradation of phenol by using tourmaline/TiO_2 system as catalyst, Adv. Mater. Res. 399–401 (2012) 1337–1341.

[12] J. Meng, J. Liang, X. Ou, Y. Ding, G. Liang, Effects of mineral tourmaline particles on the photocatalytic activity of TiO_2 thin films, J. Nanosci. Nanotechnol. 8 (2008) 1279–1283.

[13] S. Yang, Z. Wang, J. Zhao, L. Xue, C. Zhao, M. Zhao, Contrasts of structure and properties of two nano-TiO_2 wollastonite composites with wollastonite having different partical sizes, J. Jilin Uni. (Sci. Ed.) 3 (2000) 73–76.

[14] W. Sun, D. Qu, Y. Ma, Y. Chen, C. Liu, J. Zhou, Enhanced stability and antibacterial efficacy of a traditional Chinese medicine-mediated silver nanoparticle delivery system, Int. J. Nanomed. 9 (2014) 5491–5502.

[15] O. Martins, R.M. Almeida, Sintering anomaly in silica-titania sol-gel films, J. Sol-Gel Sci. Technol. 19 (2000) 651–655.

[16] W. Du, Y. Xu, Y. Wang, Photoinduced degradation of orange II on different iron (hydr)oxides in aqueous suspension: Rate enhancement on addition of hydrogen peroxide, silver nitrate, and sodium fluoride, Langmuir 24 (2008) 175–181.

[17] C.S. Turchi, D.F. Ollis, Photocatalytic degradation of organic water contaminants: Mechanisms involving hydroxyl radical attack, J. Catal. 122 (1990) 178–192.

[18] H.M. Coleman, B.R. Eggins, J.A. Byrne, F.L. Palmer, E. King, Photocatalytic degradation of 17-β-oestradiol on immobilised TiO_2, Appl. Catal. B: Environ. 24 (2000) L1–L5.

[19] B. Cui, F. Zhang, F. Cui, Q. Kong, S. Liu, Study on photocatalytic reduction of nitrate in drinking water over TiO_2 catalyst, Appl. Chem. Ind. 37 (2008) 265–267, 292.

[20] K.-H. Wang, Y.-H. Hsieh, C.-H. Wu, C.-Y. Chang, The pH and anion effects on the heterogeneous photocatalytic degradation of o-methylbenzoic acid in TiO_2 aqueous suspension, Chemosphere 40 (2000) 389–394.

[21] E. Mariquit, C. Salim, H. Hinode, The effect of calcium ions in the adsorption and photocatalytic oxidation of humic acid, J. Chem. Eng. Jpn. 42 (2009) 538–543.
[22] X.Z. Li, C.M. Fan, Y.P. Sun, Enhancement of photocatalytic oxidation of humic acid in TiO_2 suspensions by increasing cation strength, Chemosphere 48 (2002) 453–460.
[23] W. Hetterich, H. Kisch, Heterogeneous photo catalysis–VII. The influence of zinc ions on the photocatalytic properties of platinized cadmium sulfide, Photochem. Photobiol. 52 (1990) 631–635.